UNIVERSITY OF AMSTERDAM

UvA-DARE (Digital Academic Repository)

Leukocyte cathepsin S is a potent regulator of both cell and matrix turnover in advanced atherosclerosis

de Nooijer, R.; Bot, I.; von der Thüsen, J.H.; Leeuwenburgh, M.A.; Overkleeft, H.S.; Kraaijeveld, A.O.; Dorland, R.; van Santbrink, P.J.; van Heiningen, S.H.; Westra, M.M.; Kovanen, P.T.; Jukema, J.W.; van der Wall, E.E.; van Berkel, T.J.C.; Shi, G.P.; Biessen, E.A.L.

Link to publication

Leukocyte Cathepsin S Is a Potent Regulator of Both Cell and Matrix Turnover in Advanced Atherosclerosis

R. de Nooijer, I. Bot, J.H. von der Thüsen, M.A. Leeuwenburgh, H.S. Overkleeft, A.O. Kraaijeveld, R. Dorland, P.J. van Santbrink, S.H. van Heiningen, M.M. Westra, P.T. Kovanen, J.W. Jukema, E.E. van der Wall, Th.J.C. van Berkel, G.P. Shi and E.A.L. Biessen

The online version of this article, along with updated information and services, is located on the World Wide Web at:

http://atvb.ahajournals.org/cgi/content/full/29/2/188

Data Supplement (unedited) at:

http://atvb.ahajournals.org/cgi/content/full/ATVBAHA.108.181578/DC1

Subscriptions: Information about subscribing to Arteriosclerosis, Thrombosis, and Vascular Biology is online at
http://atvb.ahajournals.org/subscriptions/

Permissions: Permissions & Rights Desk, Lippincott Williams & Wilkins, a division of Wolters Kluwer Health, 351 West Camden Street, Baltimore, MD 21202-2436. Phone: 410-528-4050. Fax: 410-528-8550. E-mail:
journalpermissions@lww.com

Reprints: Information about reprints can be found online at
http://www.lww.com/reprints

Leukocyte Cathepsin S Is a Potent Regulator of Both Cell and Matrix Turnover in Advanced Atherosclerosis

R. de Nooijer, I. Bot, J.H. von der Thüsen, M.A. Leeuwenburgh, H.S. Overkleeft, A.O. Kraaijeveld, R. Dorland, P.J. van Santbrink, S.H. van Heiningen, M.M. Westra, P.T. Kovanen, J.W. Jukema, E.E. van der Wall, Th.J.C. van Berkel, G.P. Shi, E.A.L. Biessen

Objective—A dysbalance of proteases and their inhibitors is instrumental in remodeling of atherosclerotic plaques. One of the proteases implicated in matrix degradation is cathepsin-S (CatS). To address its role in advanced lesion composition, we generated chimeric LDLr$^{-/-}$ mice deficient in leukocyte CatS by transplantation with CatS$^{-/-}$×LDLr$^{-/-}$ or with LDLr$^{-/-}$ bone marrow and administered a high-fat diet.

Methods and Results—No difference in aortic root lesion size could be detected between CatS$^{+/+}$ and CatS$^{-/-}$ chimeras. However, leukocyte CatS deficiency markedly changed plaque morphology and led to a dramatic reduction in necrotic core area by 77% and an abundance of large foam cells. Plaques of CatS$^{-/-}$ chimeras contained 17% more macrophages, 62% less SMCs, and 33% less intimal collagen. The latter two could be explained by a reduced number of elastic lamina fractures. Moreover, macrophage apoptosis was reduced by 60% with CatS deficiency. In vitro, CatS was found to be involved in cholesterol metabolism and in macrophage apoptosis in a collagen and fibronectin matrix.

Conclusion—Leukocyte CatS deficiency results in considerably altered plaque morphology, with smaller necrotic cores, reduced apoptosis, and decreased SMC content and collagen deposition and may thus be critical in plaque stability. (***Arterioscler Thromb Vasc Biol***. 2009;29:188-194.)

Key Words: atherosclerosis ■ matrix ■ cathepsins ■ leukocytes ■ apoptosis

P roteolysis is an important process in the pathogenesis of atherosclerosis. Leukocyte transmigration through the endothelium, smooth muscle cell (SMC) migration through the elastic lamina, and intimal neoangiogenesis all rely on degradation of the extracellular matrix (ECM).[1–3] Proteolytic enzymes like matrix metalloproteinases (MMPs) and cathepsins have been linked to ECM remodeling leading to arterial enlargement, aneurysm formation, and plaque disruption.[4–7] Moreover, by releasing matrix-bound cytokines, chemokines, and growth factors, proteases actively participate in cell turnover and inflammation.[2,8]

Cathepsins are enzymes with strong elastolytic and collagenolytic properties and form a distinct subgroup of atherosclerosis-related proteases because their physiological actions not only affect ECM degradation, but also directly modulate inflammation, immunogenic responses, and cellular behavior.[9–12] In fact, Cathepsin-B (CatB) has been shown to activate IL-1 converting enzyme (caspase-1)[13] and Cathepsin-S (CatS) processes the invariant chain (Ii), a chaperone for MHC-II and -I, therewith affecting antigen presentation and NKT-cell maturation.[14–16]

Furthermore, CatS inhibits HDL3 induced cholesterol efflux from macrophages and several cathepsins (eg, D, F, S, and K) are able to modify apoB100 in LDL, thereby inducing foam cell formation.[17–19] CatS expression is stimulated by the proinflammatory cytokines IL-1β, IFN-γ, and TNF-α,[20] all of which have been linked to atherosclerosis.[21,22]

Because this enzyme can be expressed by all atheroma-associated cells and both its expression and activity are stimulated by a range of proinflammatory cytokines that are highly expressed in atherosclerotic plaques, Sukhova et al recently proposed the involvement of CatS in atherogenesis.[20,23–25] Also, CatS expression by macrophages at the shoulder regions was found to be increased, suggesting that this enzyme is involved in plaque rupture.[20] CatS deficiency attenuates plaque growth in LDLr knockout (LDLr$^{-/-}$) mice[26] and impairs intimal neovascularization,[27] a process that is thought to be of major importance in atherosclerotic plaque progression and stability.[28]

As CatS can exert a wide spectrum of physiological actions depending on its source, abundance, and microenvironment,

it is important to dissect the cell-specific functions of this enzyme to fully understand its role in atherogenesis. With the present study we aimed to define the leukocyte-specific function of CatS. Chimeric LDLr$^{-/-}$ mice deficient in leukocyte CatS were generated by bone marrow transplantation (BMT) of LDLr$^{-/-}$ × CatS$^{-/-}$ mice to irradiated LDLr$^{-/-}$ mice. We found that leukocyte CatS deficiency leads to a markedly altered plaque morphology and composition, which could in part be attributed to fewer elastic lamina ruptures and a higher resistance of macrophages to apoptosis and necrosis.

Materials and Methods

A detailed description of the Methods is given in the supplemental materials (available online at http://atvb.ahajournals.org).

Animals and Study Protocol

All animal work was approved by the regulatory authority of Leiden University and performed in compliance with the Dutch government guidelines. Female LDLr$^{-/-}$ mice (n=22) were obtained from our in-house breeding stock and irradiated with an X-ray dose of 9 Gy as previously described.[29] Twenty-four hours after irradiation, mice were injected intravenously with $1×10^7$ CatS-deficient bone marrow–derived cells obtained from CatS$^{-/-}$×LDLr$^{-/-}$ mice that were generated as described previously.[29] Bone marrow from CatS$^{+/+}$×LDLr$^{-/-}$ littermates was used as control. Mice were placed on a high-fat diet containing 0.25% cholesterol (Special Diet Services) for 12 weeks starting 6 weeks after BMT. After a total of 12 weeks of diet feeding, in situ perfusion-fixation was performed, after which the aortic root lesions were analyzed. Bone marrow cells were obtained for genotyping to verify that recipient cells had been replaced by donor bone marrow by flushing both femurs and tibias with PBS. Double knockout genotypes were confirmed by PCR of genomic DNA as described.[10]

Statistics

Differences in plaque size were statistically analyzed for significance using the Mann–Whitney *U* test. Other plaque parameters and constituents as well as differences in ΔCt were compared using the 2-tailed Student *t* test. The incidence of elastic lamina rupture was compared using the Yate corrected 2-sided Fisher exact test. Values are displayed as mean±SEM. A level of *P*<0.05 was considered significant.

Results

Bone Marrow Transplantation

Bone marrow transplantation was performed with freshly isolated bone marrow cells from CatS$^{-/-}$×LDLr$^{-/-}$ mice or their CatS$^{+/+}$×LDLr$^{-/-}$ littermates. Western-type diet feeding resulted in a steady elevation of plasma cholesterol levels (850±150 mg/dL to 1980±190 mg/dL) and bodyweight over a period of 12 weeks during which both parameters did not differ between groups.

To verify whether the transplantation was successful, CatS genotyping was performed on genomic DNA from bone marrow–derived cells after euthanization 18 weeks posttransplantation. This showed that CatS$^{-/-}$ BMT resulted in an almost complete depletion of autologue bone marrow (data not shown). Immunostaining revealed that the overall intimal CatS content had been reduced by approximately 50% (*P*=0.004) in CatS$^{-/-}$ transplanted animals, whereas CatS protein levels were preserved in SMC rich areas, such as the media and the fibrous cap (Figure 1A through 1C).
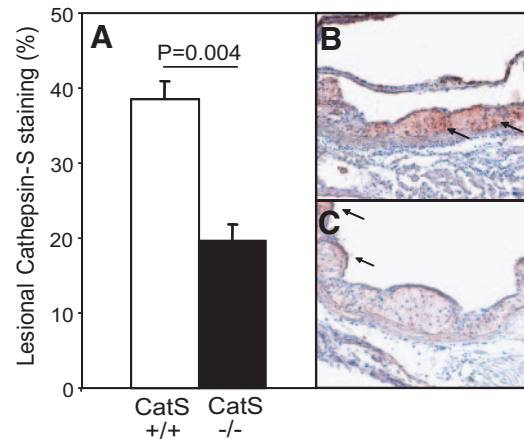

Figure 1. A, Transplantation of CatS-deficient bone marrow to irradiated recipients resulted in a 50% reduction of CatS protein levels within the atherosclerotic lesions. B, Mice that received CatS$^{+/+}$ bone marrow cells ubiquitously expressed CatS (brown staining as indicated by arrows) throughout the plaque, particularly in macrophage rich areas. C, CatS$^{-/-}$ chimerism resulted in strongly reduced intimal CatS levels. CatS expression was preserved in SMC rich areas, such as the tunica media and the fibrous cap.

No Effect on Lesion Size, but a Remarkable Change in Plaque Morphology

Advanced lesions developed within 12 weeks of high-fat diet and did not display any differences in size between both groups (Figure 2A). This study, however, aimed to analyze the effect of leukocyte CatS deficiency on the stability, morphology, and composition of advanced plaques, and this revealed a marked change in plaque phenotype. Mice with CatS deficient leukocytes tended to developed less progressed lesions compared to controls. Only 36% of the plaques in the CatS$^{-/-}$ BMT group showed a cap-core morphology compared to 82% in the control lesions (*P*=0.08, Table). Instead, the majority of these lesions were phenotypically similar to large fatty streaks, containing a high amount of macrophage derived foam cells, with few SMCs and little collagen and lacking a necrotic core with an overlying fibrous cap (Figure 2G).

Leukocyte CatS Deficiency Resulted in Decreased SMC and Collagen Content

The observed changes in plaque morphology were confirmed by quantification of several plaque constituents. Only limited amount of fibronectin could be detected in lesions by immunohistochemistry, but overall expression levels did not differ between groups (data not shown). Intimal macrophage content however was slightly increased in lesions of the CatS$^{-/-}$ chimeras (*P*=0.02), whereas SMC content was decreased by a marked 62% (*P*=0.007, Figure 2B and 2C). In keeping, intimal collagen was reduced as well (−33%, *P*=0.02), albeit that the effect was smaller than that on VSMCs (Figure 2D). In fact, the collagen:SMC-ratio increased from 2.0±0.3 in controls to 6.2±0.8 in CatS$^{-/-}$ lesion (*P*=0.03), indicating that, in addition to reduced collagen synthesis as a consequence of decreased SMC numbers, collagen degradation might be impaired as well in the absence of leukocyte CatS. Alternatively, VSMCs present in plaques of CatS$^{-/-}$ chime-
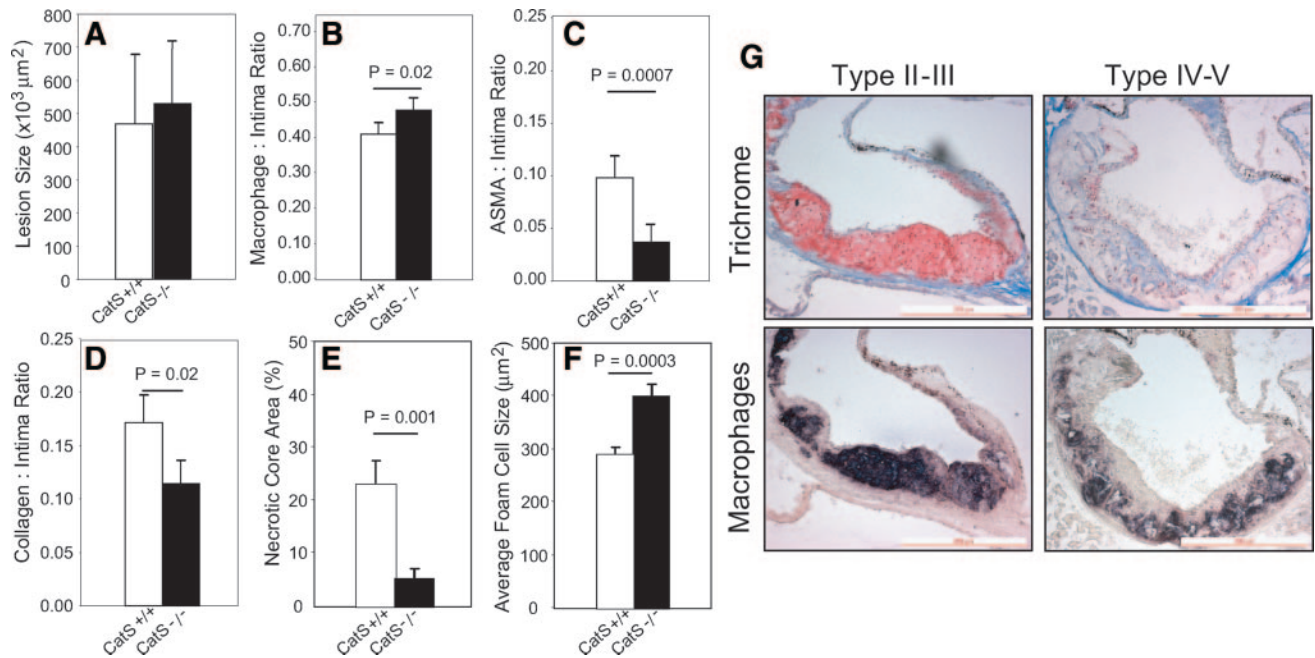
Figure 2. A, Total plaque size in the aortic root was not different between groups. B, Intimal macrophage content was moderately increased with CatS deficiency. C, Plaque content of α–SM-actin (ASMA)–positive SMCs was found to be reduced by 62% after CatS$^{-/-}$ bone marrow transplantation. D, Deposition of intimal collagen, as measured in trichrome stained sections, was reduced by 33% in the CatS$^{-/-}$ group. E, In line with the morphological features of the lesion, necrotic core area was significantly reduced after CatS$^{-/-}$ BMT. F, Foam cell size was measured in a large number of cells representative of general foam cell size within the lesion. Similar to the observed increase of foam cell type III lesions with CatS deficiency, average foam cell size was significantly increased. Values are mean±SEM. G, Typical phenotypes stained with Masson trichrome for collagen (blue staining, upper panel) and with anti-mouse macrophage antibodies (MOMA2) for macrophages (dark blue staining, lower panel). The distribution of each of these phenotypes is displayed in the Table. In the control group an advanced plaque cap-core morphology, corresponding with AHA type IV-VI lesions, could be observed in 82% of the plaques, whereas in the CatS$^{-/-}$ group this was the case in only 36%.

ras may produce more collagen, resulting in a disproportional reduction in collagen content. To test this hypothesis, collagen synthesis was determined by VSMCs in vitro in the presence or absence of CatS inhibitors. Therefore, the selective CatS inhibitor CLIK60[30] was synthesized and validated for its inhibitory capacity (supplemental Figure IA). CatS activity in RAW264.7 cells or peritoneal macrophages from C57Bl/6 or LDLr$^{-/-}$ mice was completely repressed by the specific CatS inhibitor CLIK60 at 10^{-6} mol/L. CatS inhibition by the general cathepsin inhibitor E64 as well as CLIK60 resulted in enhanced collagen synthesis, whereas Brefeldin A and serum deprivation decreased collagen synthesis as expected (supplemental Figure IB). This suggests that indeed plaque SMCs of CatS$^{-/-}$ chimeras may elaborate more collagen than SMCs in littermate plaques.

Table. Distribution of Plaque Phenotypes

	CatS$^{+/+}$	CatS$^{-/-}$	P Value
Plaque phenotype (AHA/ACC)			
Type II–III	2	7	
Type IV–VI	9	4	0.08
Foam cell size (Kawano et al[32])			
Type I	6	0	
Type II	5	7	
Type III	0	4	0.006

Leukocyte CatS Deficiency Resulted in Decreased Necrotic Core Development

Of the lesions in the CatS$^{-/-}$ chimeras, 64% did not develop necrotic cores, whereas plaques that did have smaller areas of necrosis. Necrotic core area was decreased by 77% from 22% in controls to only 5% in plaques of CatS$^{-/-}$ chimeras ($P=0.001$, Figure 2E). This effect was also observed when excluding lesions that had not developed necrotic cores at all (data not shown). Furthermore, leukocyte CatS deficiency led to lesions that contained a higher amount of large macrophage foam cells (Type III), whereas control plaques enclosed mainly small and medium sized macrophages and macrophage derived foam cells (Type I & II lesions, Table).[31] This is reflected by a 38% increase of average foam cell size ($P=0.0003$, Figure 2F).

CatS Deficiency Impaired Elastolysis and Attenuated Apoptosis

SMC content depends on a variety of factors like proliferation, migration, and ECM degradation. On stimulation SMCs will transmigrate to the intima through the elastic lamina. Degradation of the elastic lamina is vital for migration of SMCs and is mediated by the action of various proteases, such as MMP-8, CatK, and -S and to a lesser extent MMP-2 and -9. Indeed, leukocyte CatS deficiency led to a marked decrease by 68% of elastic lamina ruptures per mouse ($P=0.02$), which suggests that leukocyte-derived CatS is a
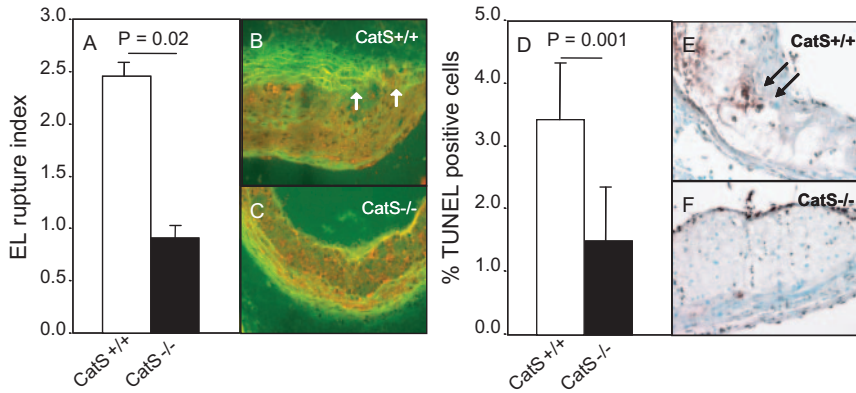
Figure 3. A through C, Impaired SMC content with leukocyte CatS could be explained by the 68% reduction of elastic lamina rupture (green fluorescent elastic lamina are visualized in B and C) in CatS$^{-/-}$ chimeras compared to control mice. Arrows indicate lamina ruptures. D through F, Decreased formation of necrotic cores with CatS deficiency could in part be explained by the 60% reduction of macrophage apoptosis as assessed with TUNEL staining. Arrows indicate brown-stained TUNEL-positive nuclei. Values are mean±SEM.

dominant elastolytic enzyme in elastic lamina disruption (Figure 3A through 3C).

As intimal macrophage content and phenotype changed on CatS deficiency and various studies have tentatively proposed a role for cathepsins in cell death,[7,12] lesions were TUNEL stained to assess apoptosis. Most commonly, TUNEL-positive staining was found in foam cell rich or necrotic areas, principally indicating macrophage cell death. In accordance with the decreased necrotic core area, apoptotic rate was reduced by approximately 60% in lesions that contained CatS deficient leukocytes ($P=0.001$; Figure 3D through 3F).

Macrophage apoptosis was further assessed in vitro. Apoptotic cell death was induced by 25 μg/mL Cu^{2+}-oxidized LDL or 10 μmol/L cisplatin. Inhibition of CatS activity did not affect RNA expression of the apoptosis related genes Bcl-2, Bax, P53, or Flip (supplemental Figure IIA). XIAP expression tended to be increased by 70%, but this was not significant ($P=0.16$). Spontaneous or oxLDL/cisplatin induced apoptotic rate measured by flow cytometry analysis of AnnexinV$^+$ cells was not affected by CLIK60 or E64 treatment, pointing to a more indirect role for CatS in apoptosis (supplemental Figure IIB).

Matrix Degradation Products and Apoptosis

To test the hypothesis that elastin degradation products, derived from CatS elastolytic activity, induced apoptosis, oxLDL-treated peritoneal macrophages were incubated with 10 μg/mL soluble elastin with or without 100 mmol/L lactose, an inhibitor of the laminin/elastin receptor. Elastin degradation products neither aggravated nor attenuated apoptotic or necrotic cell death of peritoneal macrophages nor did they affect macrophage proliferation (supplemental Figure IIC and IID).

Alternatively, CatS could effect a disruption of cell-matrix interaction of macrophages in the surrounding ECM. To test this, peritoneal macrophages were cultured on gelatin, collagen type I, or fibronectin coated dishes and stimulated with IFN-γ, a powerful CatS inducer,[20] and the effect of CLIK60 on apoptosis in this context was assessed by AnnexinV/PI staining. Cells became progressively less viable when cultured on a fibronectin or collagen matrix compared to those that were cultured on gelatin. The amount of apoptotic cells, however, remained at the level of the gelatin cultured cells, when cells were treated with CLIK60 (Figure 4), suggesting that CatS contributes to the increased apoptosis of fibronectin or collagen attached macrophages.

Furthermore, macrophages that were exposed to fibronectin displayed higher protein expression of focal adhesion kinase (FAK) compared to control cells ($P=0.01$), which was abolished when the macrophages were incubated with CatS-induced degradation products of fibronectin (supplemental Figure III). These data were confirmed by RT-PCR analysis, demonstrating that fibronectin degradation by CatS tended to reduce FAK mRNA expression compared to the expression in fibronectin exposed macrophages (relative FAK expression
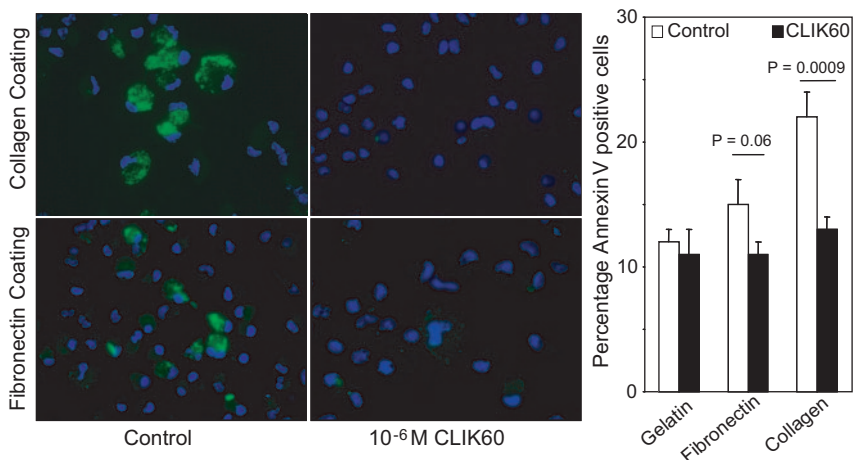
Figure 4. Peritoneal macrophages were cultured on gelatin, fibronectin, or collagen type I coated coverslips and stimulated with 400U IFNγ overnight to induce CatS expression. Apoptosis was assessed by staining externalized phosphatidylserine with AnnexinV. An increase in the amount of annexinV-positive cells on fibronectin or collagen type I coated plates could be observed as compared to cells cultured on gelatin coated dishes. This increase of apoptotic rate was prevented by selective CatS inhibition with CLIK60. Values are mean±SEM.
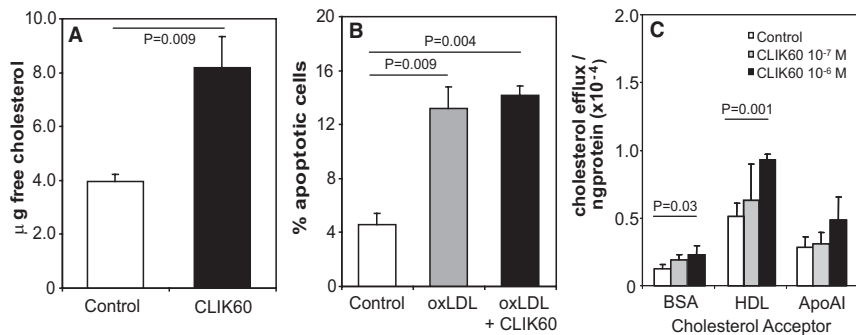
Figure 5. A, CatS inhibition by 10^{-7} mol/L CLIK60 enhanced oxLDL-induced free cholesterol accumulation in macrophages. B, 10^{-7} mol/L CLIK60 did not prevent oxLDL-induced macrophage apoptosis. C, Cholesterol efflux from peritoneal macrophages preloaded with ^{3}H-cholesterol was induced by incubation with human HDL or apoAI. Both HDL and apoAI-mediated cholesterol efflux was enhanced by CatS inhibition with CLIK60 in a dose-dependent manner. Values are mean$\pm$SEM.

0.039 ± 0.008 compared to 0.064 ± 0.002, respectively; $P=0.09$).

CatS Inhibition Increased Macrophage Cholesterol Accumulation and Efflux

As foam cells from lesions of hematopoietic CatS$^{-/-}$ chimeras were larger in size than those of littermate controls, the amount of cholesterol accumulation in macrophages was determined in vitro in the presence of CLIK60. Indeed, free cholesterol accumulation was more than 2-fold increased when CatS was inhibited by CLIK60 ($P<0.01$; Figure 5A). Because intracellular accumulation of free cholesterol has been reported to be an important inducer of apoptosis,[32] also macrophage apoptosis was determined under these conditions. As shown previously, CatS inhibition per se did not affect macrophage apoptosis (Figure 5B).

Furthermore, the effect of CatS inhibition on the cholesterol efflux capacity of peritoneal macrophages was studied. CLIK60 dose-dependently increased cholesterol efflux, enhancing HDL-induced cholesterol efflux almost 2-fold ($P=0.001$) at a concentration of 10^{-6} mol/L (Figure 5C). CatS inhibition did not affect the expression of genes involved in macrophage cholesterol metabolism, such as HMG-CoA reductase, SR-A1, SR-B1, ABCA1, and ABCG1 (data not shown). Thus, although CatS appears to be implicated in the regulation of intracellular cholesterol metabolism, a direct involvement of CatS in cholesterol-induced macrophage apoptosis could not be established. Apparently CatS may act proapoptotic in a cholesterol-independent indirect manner.

Discussion

Since the presence of CatS in human atherosclerotic plaques was first described,[20] it has become increasingly clear that it is a key actor in atherogenesis and other related vasculopathies. Given its pleiotropic actions in inflammation, cell and matrix turnover, and cholesterol trafficking, it is important to carefully map the cell specific effects of this enzyme in atherosclerosis. In this study, we specifically establish the role of leukocyte CatS in atherosclerotic plaque composition. Cellular and matrix composition of advanced plaques was dramatically altered in mice that were transplanted with CatS-deficient bone marrow, showing a 62% decrease of SMC content, which could, at least in part, be explained by a marked decrease in elastic lamina ruptures, pivotal for SMC migration into the intima. The disproportional reduction of intimal collagen by only 33% suggests that CatS may also be directly involved in intimal collagen production and break-

down. Previous studies with CatS$^{-/-}$ mice already showed impaired lamina degradation and reduced intimal SMC and collagen content.[26] Rodgers et al have recently demonstrated that CatS contributes significantly to plaque progression as demonstrated by a reduced plaque size and a reduced number of fibrous cap ruptures in apoE/CatS double knockout mice. Collagen levels and the number of elastic lamina ruptures remained unaffected by CatS deficiency.[33] The present study establishes that leukocyte-, and not SMC-, derived CatS is instrumental in the degradation of the inner elastic lamina, which renders leukocyte CatS a potential target for plaque stabilization. Elastin degradation products have previously been reported to be able to promote SMC proliferation via the elastin/laminin receptor.[34] Conceivably, in our study, the absence of the elastolytic CatS might have contributed to impaired intimal SMC accumulation. However, no effect of degraded elastin could be detected on macrophage proliferation, nor was there any effect of elastin degradation products on apoptosis, either spontaneous or induced with oxLDL or cisplatin.

Earlier studies demonstrated that systemic CatS deficiency impairs monocyte transmigration through an endothelial barrier.[26] By contrast, monocyte infiltration was not repressed and lesional macrophage staining area was even increased in the absence of leukocyte CatS. Thus, whereas earlier studies showed impaired monocyte transmigration through the endothelium in CatS$^{-/-}$ mice,[26] the present observations suggest that endothelial cell–, and not monocyte-, derived CatS is vital for leukocyte transmigration. The relative increase of intimal macrophages and the observed higher abundance of large foam cells could be explained by the vast reduction in necrotic core formation and reduced susceptibility of macrophages to apoptosis in the absence of CatS.

Several studies show that lysosomal enzymes, including Cathepsin B, D, and L, can directly induce apoptosis once released from the lysosomal compartment.[12,35–37] We now show that CatS inhibition by CLIK60 did not directly affect apoptosis or necrosis in macrophages that were stimulated with oxLDL or cisplatin. Moreover, the expression levels of several apoptosis-related genes remained unaffected by CLIK60. Additionally, ECM constituents and degradation products have been reported to be important regulators of cell death.[7,37,38] As mentioned earlier, soluble elastin degradation products did not affect apoptosis or proliferation of macrophages in vitro. Interestingly, macrophages cultured on fibronectin or collagen type I showed an increased apoptotic

rate compared to macrophages that were cultured on gelatin. Inhibition of CatS activity prevented this induction of apoptosis and kept the rate of cell death at the baseline level of gelatin cultured macrophages. In vivo, fibronectin levels may be affected with reduced plaque CatS content, however only limited amount of fibronectin was detectable in atherosclerotic lesions and despite reduced lesional CatS content overall plaque fibronectin did not differ between groups. However, the in vitro data suggest that CatS may induce apoptosis by mediating pericellular fibronectin and collagen type I breakdown and may thus be an important regulator of macrophage apoptosis in vivo. These effects may be, at least partially, attributable to loss of FAK expression induced after CatS mediated degradation of fibronectin, resulting in detachment of macrophages from the extracellular matrix.

Finally, free cholesterol is a potent inducer of apoptosis in macrophages by triggering cytochrome C release and activating FasL.[32,39,40] In line with earlier observations regarding the inhibitory action of CatS on cholesterol efflux,[17] CatS inhibition was indeed found to potentiate both HDL and apoAI-induced cholesterol efflux from peritoneal macrophages. Intriguingly, CatS inhibition also led to enhanced free cholesterol accumulation, which did not affect macrophage apoptosis, pointing toward a more indirect role for CatS in the regulation of apoptosis.

In conclusion, our data suggest that leukocytic CatS contributes to plaque growth and stability. Medial SMC migration into the intima and subsequent proliferation and collagen deposition heavily relies on the elastolytic properties of macrophage derived CatS. Also, the critical contribution of macrophage CatS to necrotic core expansion in advanced plaques underpins its importance for plaque stability and eventually acute ischemic events.

Sources of Funding

Disclosures

None.

References

1. Katsuda S, Kaji T. Atherosclerosis and extracellular matrix. *J Atheroscler Thromb*. 2003;10:267–274.
2. Bergers G, Brekken R, McMahon G, Vu TH, Itoh T, Tamaki K, Tanzawa K, Thorpe P, Itohara S, Werb Z, Hanahan D. Matrix metalloproteinase-9 triggers the angiogenic switch during carcinogenesis. *Nat Cell Biol*. 2000;2:737–744.
3. Garcia-Touchard A, Henry TD, Sangiorgi G, Spagnoli LG, Mauriello A, Conover C, Schwartz RS. Extracellular proteases in atherosclerosis and restenosis. *Arterioscler Thromb Vasc Biol*. 2005;25:1119–1127.
4. Luttun A, Carmeliet P. Genetic studies on the role of proteinases and growth factors in atherosclerosis and aneurysm formation. *Ann N Y Acad Sci*. 2001;947:124–132.
5. Freestone T, Turner RJ, Coady A, Higman DJ, Greenhalgh RM, Powell JT. Inflammation and matrix metalloproteinases in the enlarging abdominal aortic aneurysm. *Arterioscler Thromb Vasc Biol*. 1995;15: 1145–1151.
6. Newby AC. Dual role of matrix metalloproteinases (matrixins) in intimal thickening and atherosclerotic plaque rupture. *Physiol Rev*. 2005;85:1–31.
7. Lindstedt KA, Leskinen MJ, Kovanen PT. Proteolysis of the pericellular matrix: a novel element determining cell survival and death in the pathogenesis of plaque erosion and rupture. *Arterioscler Thromb Vasc Biol*. 2004;24:1350–1358.
8. Belotti D, Paganoni P, Manenti L, Garofalo A, Marchini S, Taraboletti G, Giavazzi R. Matrix metalloproteinases (MMP9 and MMP2) induce the release of vascular endothelial growth factor (VEGF) by ovarian carcinoma cells: implications for ascites formation. *Cancer Res*. 2003;63: 5224–5229.
9. Riese RJ, Mitchell RN, Villadangos JA, Shi GP, Palmer JT, Karp ER, De Sanctis GT, Ploegh HL, Chapman HA. Cathepsin S activity regulates antigen presentation and immunity. *J Clin Invest*. 1998;101:2351–2363.
10. Shi GP, Villadangos JA, Dranoff G, Small C, Gu L, Haley KJ, Riese R, Ploegh HL, Chapman HA. Cathepsin S required for normal MHC class II peptide loading and germinal center development. *Immunity*. 1999;10: 197–206.
11. Shi GP, Bryant RA, Riese R, Verhelst S, Driessen C, Li Z, Bromme D, Ploegh HL, Chapman HA. Role for cathepsin F in invariant chain processing and major histocompatibility complex class II peptide loading by macrophages. *J Exp Med*. 2000;191:1177–1186.
12. Li W, Yuan XM. Increased expression and translocation of lysosomal cathepsins contribute to macrophage apoptosis in atherogenesis. *Ann N Y Acad Sci*. 2004;1030:427–433.
13. Hentze H, Lin XY, Choi MS, Porter AG. Critical role for cathepsin B in mediating caspase-1-dependent interleukin-18 maturation and caspase-1-independent necrosis triggered by the microbial toxin nigericin. *Cell Death Differ*. 2003;10:956–968.
14. Liu W, Spero DM. Cysteine protease cathepsin S as a key step in antigen presentation. *Drug News Perspect*. 2004;17:357–363.
15. Riese RJ, Shi GP, Villadangos J, Stetson D, Driessen C, Lennon-Dumenil AM, Chu CL, Naumov Y, Behar SM, Ploegh H, Locksley R, Chapman HA. Regulation of CD1 function and NK1.1(+) T cell selection and maturation by cathepsin S. *Immunity*. 2001;15:909–919.
16. Driessen C, Bryant RA, Lennon-Duménil AM, Villadangos JA, Bryant PW, Shi GP, Chapman HA, Ploegh HL. Cathepsin S controls the trafficking and maturation of MHC class II molecules in dendritic cells. *J Cell Biol*. 1999;147:775–790.
17. Lindstedt L, Lee M, Oörni K, Brömme D, Kovanen PT. Cathepsins F and S block HDL3-induced cholesterol efflux from macrophage foam cells. *Biochem Biophys Res Commun*. 2003;312:1019–1024.
18. Hakala JK, Oksjoki R, Laine P, Du H, Grabowski GA, Kovanen PT, Pentikäinen MO. Lysosomal enzymes are released from cultured human macrophages, hydrolyze LDL in vitro, and are present extracellularly in human atherosclerotic lesions. *Arterioscler Thromb Vasc Biol*. 2003;23: 1430–1436.
19. Camejo G. Hydrolytic enzymes released from resident macrophages and located in the intima extracellular matrix as agents that modify retained apolipoprotein B lipoproteins. *Arterioscler Thromb Vasc Biol*. 2003;23: 1312–1313.
20. Sukhova GK, Shi GP, Simon DI, Chapman HA, Libby P. Expression of the elastolytic cathepsins S and K in human atheroma and regulation of their production in smooth muscle cells. *J Clin Invest*. 1998;102: 576–583.
21. Whitman SC, Ravisankar P, Elam H, Daugherty A. Exogenous interferon-gamma enhances atherosclerosis in apolipoprotein E$^{-/-}$ mice. *Am J Pathol*. 2000;157:1819–1824.
22. Tellides G, Tereb DA, Kirkiles-Smith NC, Kim RW, Wilson JH, Schechner JS, Lorber MI, Pober JS. Interferon-gamma elicits arteriosclerosis in the absence of leukocytes. *Nature*. 2000;403:207–211.
23. Storm van's Gravesande K, Layne MD, Ye Q, Le L, Baron RM, Perrella MA, Santambrogio L, Silverman ES, Riese RJ. IFN regulatory factor-1 regulates IFN-gamma-dependent cathepsin S expression. *J Immunol*. 2002;168:4488–4494.
24. Cheng XW, Kuzuya M, Sasaki T, Arakawa K, Kanda S, Sumi D, Koike T, Maeda K, Tamaya-Mori N, Shi GP, Saito N, Iguchi A. Increased expression of elastolytic cysteine proteases, cathepsins S and K, in the neointima of balloon-injured rat carotid arteries. *Am J Pathol*. 2004;164: 243–251.
25. Jormsjö S, Wuttge DM, Sirsjö A, Whatling C, Hamsten A, Stemme S, Eriksson P. Differential expression of cysteine and aspartic proteases

during progression of atherosclerosis in apolipoprotein E-deficient mice. *Am J Pathol*. 2002;161:939–945.

26. Sukhova GK, Zhang Y, Pan JH, Wada Y, Yamamoto T, Naito M, Kodama T, Tsimikas S, Witztum JL, Lu ML, Sakara Y, Chin MT, Libby P, Shi GP. Deficiency of cathepsin S reduces atherosclerosis in LDL receptor-deficient mice. *J Clin Invest*. 2003;111:897–906.

27. Shi GP, Sukhova GK, Kuzuya M, Ye Q, Du J, Zhang Y, Pan JH, Lu ML, Cheng XW, Iguchi A, Perrey S, Lee AM, Chapman HA, Libby P. Deficiency of the cysteine protease cathepsin S impairs microvessel growth. *Circ Res*. 2003;92:493–500.

28. Celletti FL, Waugh JM, Amabile PG, Brendolan A, Hilfiker PR, Dake MD. Vascular endothelial growth factor enhances atherosclerotic plaque progression. *Nat Med*. 2001;7:425–429.

29. Van Eck M, Bos IS, Kaminski WE, Orsó E, Rothe G, Twisk J, Böttcher A, Van Amersfoort ES, Christiansen-Weber TA, Fung-Leung WP, Van Berkel TJ, Schmitz G. Leukocyte ABCA1 controls susceptibility to atherosclerosis and macrophage recruitment into tissues. *Proc Natl Acad Sci U S A*. 2002;99:6298–6303.

30. Katunuma N, Tsuge H, Nukatsuka M, Asao T, Fukushima M. Structure-based design of specific cathepsin inhibitors and their application to protection of bone metastases of cancer cells. *Arch Biochem Biophys*. 2002;397:305–311.

31. Kawano H, Yano T, Mizuguchi K, Mochizuki H, Saito Y. Changes in aspects such as the collagenous fiber density and foam cell size of atherosclerotic lesions composed of foam cells, smooth muscle cells and fibrous components in rabbits caused by all-cis-5, 8, 11, 14, 17-icosapentaenoic acid. *J Atheroscler Thromb*. 2002;9:170–177.

32. Tabas I Apoptosis and plaque destabilization in atherosclerosis: the role of macrophage apoptosis induced by cholesterol. *Cell Death Differ*. 2004;11 Suppl 1:S12–S16.

33. Rodgers KJ, Watkins DJ, Miller AL, Chan PY, Karanam S, Brissette WH, Long CJ, Jackson CL. Destabilizing role of cathepsin S in murine atherosclerotic plaques. *Arterioscler Thromb Vasc Biol*. 2006;26:851–856.

34. Mochizuki S, Brassart B, Hinek A. Signaling pathways transduced through the elastin receptor facilitate proliferation of arterial smooth muscle cells. *J Biol Chem*. 2002;277:44854–44863.

35. Li W, Yuan XM, Olsson AG, Brunk UT. Uptake of oxidized LDL by macrophages results in partial lysosomal enzyme inactivation and relocation. *Arterioscler Thromb Vasc Biol*. 1998;18:177–184.

36. Li W, Dalen H, Eaton JW, Yuan XM. Apoptotic death of inflammatory cells in human atheroma. *Arterioscler Thromb Vasc Biol*. 2001;21:1124–1130.

37. Michel JB. Anoikis in the cardiovascular system: known and unknown extracellular mediators. *Arterioscler Thromb Vasc Biol*. 2003;23:2146–2154.

38. Meilhac O, Ho-Tin-Noé B, Houard X, Philippe M, Michel JB, Anglés-Cano E. Pericellular plasmin induces smooth muscle cell anoikis. *Faseb J*. 2003;17:1301–1303.

39. Yao PM, Tabas I. Free cholesterol loading of macrophages is associated with widespread mitochondrial dysfunction and activation of the mitochondrial apoptosis pathway. *J Biol Chem*. 2001;276:42468–42476.

40. Yao PM, Tabas I. Free cholesterol loading of macrophages induces apoptosis involving the fas pathway. *J Biol Chem*. 2000;275:23807–23813.

Additional Figures

Online Figure 1
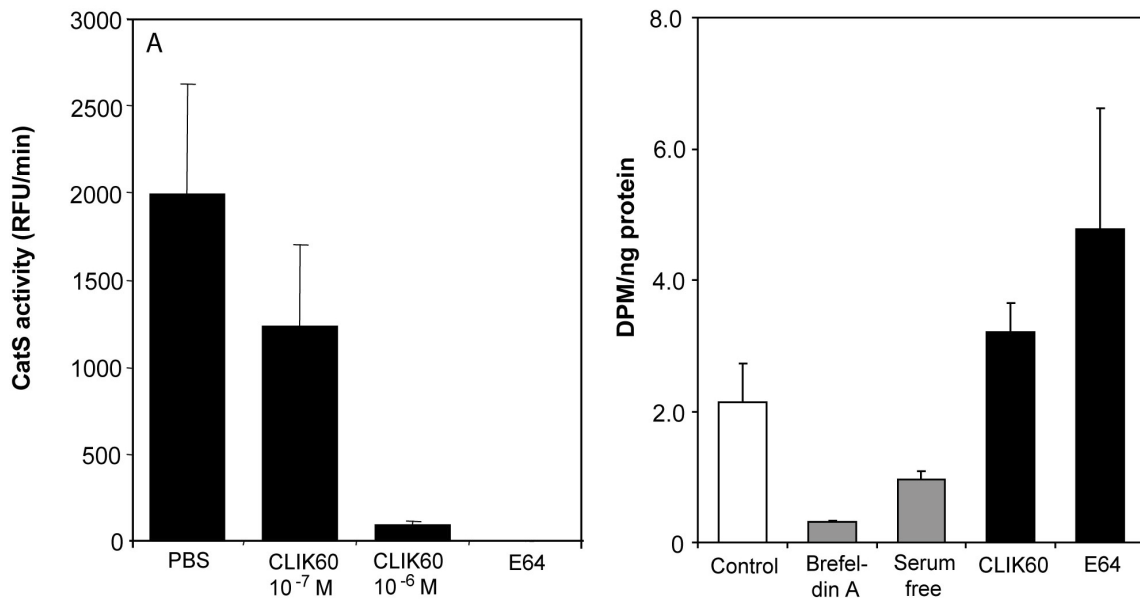
Online Figure 1. **A.** The selective CatS inhibitor CLIK60 dose-dependently inhibited cathepsin S activity. CatS activity in RAW264.7 cells or peritoneal macrophages from C57Bl/6 or LDLr$^{-/-}$ mice was almost completely repressed by CLIK60 at 10^{-6}M. **B.** Inhibition of CatS by 10^{-7} M CLIK60 or 10 μM E64 did not inhibit but enhanced collagen production by SMCs *in vitro*, while the controls Brefeldin A and serum deprivation resulted in reduced collagen levels in these cells. Values are mean ± SEM.

Online Figure 2
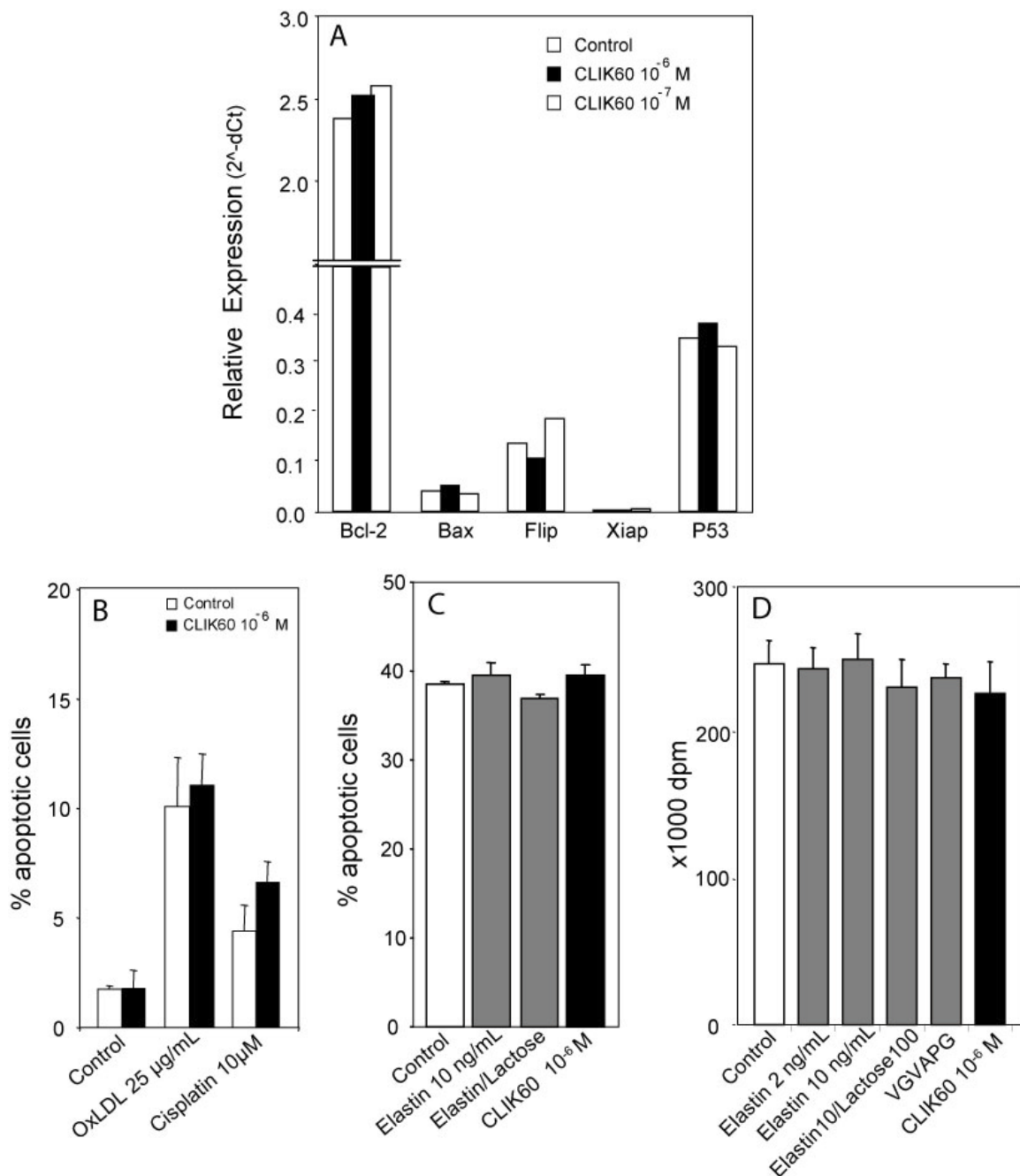
Online Figure 2. A. Inhibition of CatS activity did not affect macrophage RNA expression of the apoptosis related genes Bcl-2, Bax, P53 or Flip, while XIAP expression tended to be increased. **B.** OxLDL or cisplatin induced macrophage apoptosis was not

affected by CLIK60. **C, D.** Elastin degradation products neither aggravated nor attenuated apoptotic or necrotic cell death of peritoneal macrophages nor did they affect macrophage proliferation, which were also not affected by CLIK60. Values are mean ± SEM.

Online Figure 3
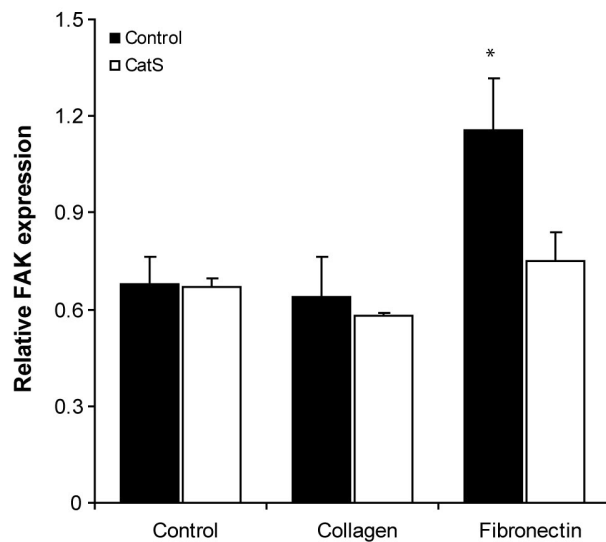
Online Figure 3. Focal Adhesion Kinase (FAK) protein expression relative to tubulin, demonstrating that fibronectin enhanced FAK expression in the macrophage cell line RAW264.7, which does not occur when these cells were exposed to CatS derived degradation products of fibronectin. CatS conditioned medium, which was inactivated with 10% FCS before application to the cells, did not affect FAK expression, while also collagen and collagen degradation products were ineffective in altering FAK protein expression.

Expanded Materials and Methods

Animals and study protocol

All animal work was approved by the regulatory authority of Leiden University and performed in compliance with the Dutch government guidelines. Female LDL receptor deficient mice (LDLr$^{-/-}$, n=22), 20-24 weeks of age, were obtained from our in-house breeding stock and irradiated with an X-ray dose of 9 Gy as previously described[1]. Twenty-four hours after irradiation, mice were injected intravenously with $1 \cdot 10^7$ CatS deficient bone marrow derived cells obtained from CatS$^{-/-}$ x LDLr$^{-/-}$ mice that were generated as previously described[1]. Bone marrow from CatS$^{+/+}$ x LDLr$^{-/-}$ littermates was used as control. Mice were placed on a high-fat diet containing 0.25% cholesterol (Special Diet Services, UK) for 12 weeks starting 6 weeks after BMT. Concentrations of plasma cholesterol were determined every 14 days by enzymatic procedures (Boehringer Mannheim, Germany). Precipath (standardized serum; Boehringer Mannheim, Germany) was used as an internal standard. After a total of 12 weeks of diet feeding, *in situ* perfusion-fixation was performed, after which the aortic root lesions were analyzed. Bone marrow cells were obtained for genotyping to verify that recipient cells had been replaced by donor bone marrow by flushing both femurs and tibias with PBS. Double knockout genotypes were confirmed by PCR of genomic DNA as described[2,3].

Histological analysis

Serial cryosections were prepared from OCT-embedded aortic roots (10 μm thickness) and routinely stained with hematoxylin (Sigma) and eosin (Merck), Oil-Red-O (Sigma) and with Masson's trichrome (Sigma). Five Oil-Red-O stained sections per

mouse were selected for morphometry, digitized and analyzed as previously described[4]. Corresponding sections were stained with antibodies directed against mouse metallophilic macrophages (MOMA2; Sigma) and α-SM-actin (1A4; Sigma) and cathepsin-S[2]. CatS, Macrophage, SMC and collagen positive areas were determined by computer-assisted color-gated measurement, and related to the total intimal surface area (Leica QWin). Lesions were classified according to average foam cell size: Type I lesions contain no or small foam cells, Type II reflects plaques that mostly enclose small, but also few large foam cells, while type III lesions are mostly constituted of large foam cells[5]. Necrotic core was defined as the a-cellular, debris-rich plaque area as percentage of total plaque area, quantified with Leica QWin software. The elastic lamina was visualized by autofluorescence on Oil Red O stained sections and lamina degradation was expressed as number of ruptures per mouse. To assess intimal cell death, sections were subjected to TUNEL staining according to manufacturer instructions (Roche Diagnostics). TUNEL positive cells, showing cell shrinkage, membrane blebbing or nuclear condensation[6], were counted and related to the total number of intimal cells. Fibronectin staining was performed as follows. Sections were blocked with Vector Vectastain rabbit-kit for 30 minutes, after which the slides were incubated overnight at 4°C with a rabbit-anti-mouse fibronectin (Sigma F3648) antibody 1:100 in 3% normal goat serum in PBS. Subsequently, the sections were incubated with a biotinylated secondary antibody from Vectastain kit for 30 minutes, and fibronectin visualized by incubation with ABC-reagent for 40 minutes and AEC (3'amino-9'ethylcarbatsole) for 8-10 minutes. Sections were couterstained with Mayer's hematoxylin.

Synthesis of CLIK60 and CatS activity assay

To inhibit CatS activity, the selective CatS inhibitor CLIK60 was prepared according to procedures described by Katunuma *et al*. and had nuclear magnetic resonance, infrared and mass spectra consistent with the structure of the compound[7]. The purity was determined to be >97% by HPLC analysis. CLIK60 has been reported to inhibit 100% of CatS activity at 10^{-6} M and 86% at 10^{-7} M and shows virtually no inhibition of other cathepsins[7].

Cathepsin S activity was measured using the internally quenched fluorogenic peptide substrate Z-Phe-Val-Arg-AMC. Cell lysate samples were 10-fold diluted in CatS buffer (200 mM Na Acetate buffer pH 5.5, 4 mM EDTA, 8 mM DTT in 0.1% CHAPS). Conversion of the substrate was assessed in presence or absence of 10 µM E64, a general cathepsin inhibitor, or various concentrations of CLIK60. The initial rate of substrate conversion was used as a measure of cathepsin S activity. AMC release was measured in real-time for 30 min at 28°C using a fluorescence plate reader.

Cell culture

Peritoneal macrophages were isolated from C57Bl/6 mice, as described previously[8]. Briefly, mice were injected intraperitoneally with 1 mL sterile 3% (w/v) Brewer's thioglycollate. On day 5, peritoneal cells were harvested, washed, and resuspended in standard medium (Dulbecco's modified Eagle's medium, PAA, Cölbe, Germany) containing 20 mM HEPES, 4 mM glutamine, penicillin-streptomycin solution and 10% FCS. Cells were seeded into 0.1% gelatin-coated 24-wells tissue-culture plates

($5.0 \cdot 10^5$ cells/well) and incubated at 37°C for 4 h to allow cells to adhere. Non-adherent cells were removed, and remaining cells were re-fed with standard medium.

The murine macrophage cell line RAW 264.7 and primary vascular smooth muscle cells (vSMCS), isolated from mouse aortas as described previously[9], were cultured in DMEM containing 10% Fetal Bovine Serum (FBS), 2 mmol/L l-glutamine, 100 U/mL penicillin, and 100 µg/mL streptomycin in a humidified atmosphere (5% CO_2) and at 37°C.

Apoptosis and proliferation experiments

After an 8h pre-incubation with soluble elastin (1-10 ng/mL) +/- lactose (100 mM), an inhibitor of the elastin receptor[10], or with CLIK60 ($10^{-6}/10^{-7}$ M), peritoneal macrophages and RAW264.7 cells were incubated for 18h - in the presence of above mentioned vehicles - with 10 µM cisplatin or 25 µg/mL oxLDL to induce apoptosis. To assess cell death, cells were gently washed with PBS/1 mM EDTA, brought into suspension and washed once more in standard medium. Externalized phosphatidylserine was labeled (15 min at 0°C) with AnnexinV (1 mg/mL; Santa Cruz) in AV buffer (10 mM HEPES, 145 mM NaCl, 5 mM KCl, 1.0 mM $MgCl_2$, 1.8 mM $CaCl_2$; pH 7.4). Propidium iodide (3.3 µM) in AV buffer was added 1 min before analysis by flow cytometry on a FACScalibur (Becton Dickinson). Similarly, RAW264.7 cells were incubated for 18 hours with 25 µg/mL oxLDL with or without 10^{-7} M CLIK60, after which the rate of apoptosis was measured as described above. In addition, IFNγ (400 U) stimulated peritoneal macrophages were incubated for 48 h with or without 10^{-6} M CLIK60 on gelatin (0.1%), collagen type I (0.1%) or fibronectin (0.1%) coated cover

slips. Cells were visualized with Hoechst 33258 and Annexin V by fluorescence microscopy.

To examine the effect of CatS inhibition on proliferation, RAW264.7 cells were cultured in 24-well dishes, synchronized by culturing in serum-free media overnight and in standard culture media for an additional day. Proliferation rate was quantified by adding 1 µCi ^{3}H-thymidine per mL culture medium and measuring uptake over 5 h.

Collagen synthesis assay

To measure collagen synthesis, 24-well dishes were incubated for 20 minutes with 1 mg/mL collagen type I, after which vSMCs were plated at a density of $1*10^6$ cells/well. After adherence, cells were exposed to CLIK60 (0.1 and 1 µM), E64 (10 µM) or Brefeldin A (1 µM). As negative control, cells were serum deprived. [^{3}H]-proline (1.0 µCi/well) and ascorbic acid (50 µg/mL) were added as well and cells were incubated overnight at 37°C. Next, cells were washed with PBS and with 20 mM Tris-HCl (pH=7.6), after which they were suspended in 500 µL 20 mM Tris.HCl/0.36 mM CaCL$_2$ (pH=7.6) and sonicated for 45 seconds. The samples were incubated with collagenase (100 U/mL) for 2 hours at 37°C, after which non-collagen proteins were precipitated with 100 µL 50% TCA. Supernatants were measured for radioactivity.

Expression analysis

Peritoneal macrophages were incubated with CLIK60 (10^{-6} M) for 18h and RNA was isolated using the TRIZOL method (Invitrogen, Netherlands) according to the manufacturer's instructions. Purified RNA was reverse transcribed (RevertAid M-MulV)

according to the protocols provided by the manufacturer. Quantitative gene expression analysis was performed on an ABI PRISM 7700 machine (Applied Biosystems, Foster City, CA) using SYBR Green technology. Primers were designed for murine Bax, Bcl-2, XIAP, Flip, p53, SRA, SRBI, ABCA1, ABCG1 and HMGCoA using PrimerExpress 1.7 (Applied Biosystems) and validated for identical efficiencies. Target gene mRNA levels were expressed relative to that of the housekeeping gene (36b4) and calculated by subtracting the threshold cycle number (Ct) of the target gene from the Ct of 36b4 and raising two to the power of this difference.

To assess the effects of CatS mediated matrix degradation on the expression of Focal Adhesion Kinase (FAK), collagen type 1 (1 mg/mL) or fibronectin (5 μg/mL) were incubated overnight at 37°C in serum-free medium in the presence or absence of 500 ng/mL CatS (human spleen, VWR). The next day, CatS was inactivated by addition of 10 % FCS and the conditioned medium was applied to RAW264.7 cells (100.000 cells/well) and incubated overnight at 37°C. The next day, cells were either lysed for protein or for mRNA analysis. Protein expression was analyzed by Western blotting using mouse anti-FAK, clone 4.47 (Upstate Biotech, Charlottesville, VA, USA) primary antibody and rabbit anti-mouse-HRP (Dako) secondary antibody.

Total RNA was extracted and FAK gene expression was analyzed by quantitative real-time PCR as described above and the following primers were used: forward 5'GAGAATCCAGCTTTGGCTGTT3', reverse 5'GGCTTCTTGAAGGAACTTCT3'. Hypoxanthine-guanine phosphoribosyltransferase (HPRT, forward: 5'TTGCTCGA-GATGTCATGAAGGA3', reverse: 5'AGCAGGTCAGCAAAGAACTTATAG3') was used as house-keeping gene.

Cholesterol accumulation and efflux

To assess whether CatS inhibition affected cholesterol accumulation, $1*10^5$ RAW264.7 cells were incubated for 18 hours with 25 µg/mL oxLDL with or without 10^{-7} M CLIK60. Cells were lysed with 0.1 M NaOH, after which free cholesterol levels were determined by enzymatic procedures (Boehringer Mannheim). Precipath (standardized serum; Boehringer Mannheim) was used as an internal standard.

Peritoneal macrophages were stimulated with 400U IFNγ and incubated with or without CLIK60 (10^{-6}/10^{-7} M) throughout the experiment. After an 18 h incubation, cells were loaded with 3 mg/mL cholesterol and 1 mg/mL ^{3}H-cholesterol (0.5 µCi/mL) in standard culture medium containing 10% BSA during the next 24 h and equilibrated in cholesterol-free media for another 24 h. Cholesterol efflux was induced by addition of human HDL (50 µg/mL) or ApoAI (5 µg/mL) or BSA as a control. Total amount of efflux was measured by LCS analysis of cell lysate and supernatant after 24 h.

Statistics

Differences in plaque size were statistically analyzed for significance using the Mann-Whitney U test. Other plaque parameters and constituents as well as differences in ΔCt were compared using the two-tailed Student's *t*-test. The incidence of elastic lamina rupture was compared using the Yate's corrected two-sided Fisher exact test. Values are displayed as mean ± SEM. A level of *P*<0.05 was considered significant.

Refences

1. Van Eck M, Bos IS, Kaminski WE, Orsó E, Rothe G, Twisk J, Böttcher A, Van Amersfoort ES, Christiansen-Weber TA, Fung-Leung WP, Van Berkel TJ, Schmitz G. Leukocyte ABCA1 controls susceptibility to atherosclerosis and macrophage recruitment into tissues. Proc Natl Acad Sci U S A. 2002;99:6298-6303.

2. Shi GP, Villadangos JA, Dranoff G, Small C, Gu L, Haley KJ, Riese R, Ploegh HL, Chapman HA. Cathepsin S required for normal MHC class II peptide loading and germinal center development. Immunity. 1999;10:197-206.

3. Ishibashi S, Brown MS, Goldstein JL, Gerard RD, Hammer RE, Herz J. Hypercholesterolemia in low density lipoprotein receptor knockout mice and its reversal by adenovirus-mediated gene delivery. J Clin Invest. 1993;92:883-893.

4. von der Thüsen JH, van Vlijmen BJ, Hoeben RC, Kockx MM, Havekes LM, van Berkel TJ, Biessen EA. Induction of atherosclerotic plaque rupture in apolipoprotein E-/- mice after adenovirus-mediated transfer of p53. Circulation. 2002;105:2064-2070.

5. Kawano H, Yano T, Mizuguchi K, Mochizuki H, Saito Y. Changes in aspects such as the collagenous fiber density and foam cell size of atherosclerotic lesions composed of foam cells, smooth muscle cells and fibrous components in rabbits caused by all-cis-5, 8, 11, 14, 17-icosapentaenoic acid. J Atheroscler Thromb. 2002;9:170-177.

6. Kockx MM. Apoptosis in the atherosclerotic plaque: quantitative and qualitative aspects. Arterioscler Thromb Vasc Biol. 1998;18:1519-1522.

7. Katunuma N, Tsuge H, Nukatsuka M, Asao T, Fukushima M. Structure-based design of specific cathepsin inhibitors and their application to protection of bone metastases of cancer cells. Arch Biochem Biophys. 2002;397:305-311.

8. Herijgers N, Van Eck M, Groot PH, Hoogerbrugge PM, Van Berkel TJ. Low density lipoprotein receptor of macrophages facilitates atherosclerotic lesion formation in C57Bl/6 mice. Arterioscler Thromb Vasc Biol. 2000;20:1961-1967.

9. Michon IN, Hauer AD, von der Thüsen JH, Molenaar TJM, van Berkel TJC, Biessen EAL, Kuiper J. Targeting of peptides to restenotic vascular smooth muscle cells using phage display in vitro and in vivo. Biochim Biophys Acta. 2002;1591:87-97.

10. Faury G, Usson Y, Robert-Nicoud M, Robert L, Verdetti J. Nuclear and cytoplasmic free calcium level changes induced by elastin peptides in human endothelial cells. Proc Natl Acad Sci U S A. 1998;95:2967-2972.